Flow Control in an Open Channel by Skewed Strip Roughness

Supervisor: Prof. Akihiro TOMINAGA NYARSUK Robert Lado Wurda

1. Introduction. The research on turbulent flow over strip roughness is generally looked upon as one of the most basic approaches to understand the generation mechanism of turbulence in the flow over rough boundary. The generation of secondary flow and the resistance to the mainflow in an open channel can be highly influenced by the shape, size, spacing and arrangement of the roughness elements installed in the channel. The secondary currents generated due to roughness elements can be used to control flow in an open channel. This experiment focuses on the influence of the oblique shoulders of the roughness elements on flow resistance, sediment transport and controlling the zone of sediment transport and deposition in open channel flow.

2. Methodology. The experiment was conducted in a flume of 7.5m in length, 0.3m in width and 0.4m in height. The strips of acrylic resin with 5mm x 5mm cross sectional area were placed on the bed of the flume in the spanwise direction at 20cm interval. Three different arrangements of the roughness elements were considered, (H-type, A-type and V-type). The strips were skewed at an angle with respect to the spanwise direction as shown in Fig.1. To avoid flow stagnation at the center and near wall region, the strips were aligned such that there is constant smooth bed before and after each strip along the width of the channel (a=5cm) giving a uniform projection area of 7.5cm in all cases. For full development of turbulence, the strips covered 3m of the total length of the flume starting 1.5m downstream of the flow entrance. Three skew angles were considered in both A-type and V-type arrangement of the roughness elements. PIV experiment was use for the velocity measurements. 7sections at 5mm interval and 11sections at 30mm interval were measure in the horizontal and vertical velocity measurements respectively. Two sets of velocities (U, V) and (U, W) were obtained experimentally and integrated in to three velocity components (U, V and W). For visualization of the flow, nylon resin particles with 80 microns in diameter and specific weight of 1.02 were used. The visual images were taken by a high-speed video camera with 200 frames per second and they were recorded as AVI files with 1024 x 1024 pixels. Flowexpert software was used in the velocity analysis.

Table 1 Hydraulic conditions

	Discharge Q(L/s)	Mean Velocity Um(cm/s)	Water depth h(cm)	Fr	Slope I
PIV	3.00	25.00	4.00	0.40	1/1000
Sediment Transport	3.60	30.00		0.48	

Table 2 Model setup

case	H1	A1	A2	A3
		V1	V2	V3
k(cm)	0.5			
L(cm)	20			
a(cm)	5			
B(cm)	30			
θ°	0	30	45	60

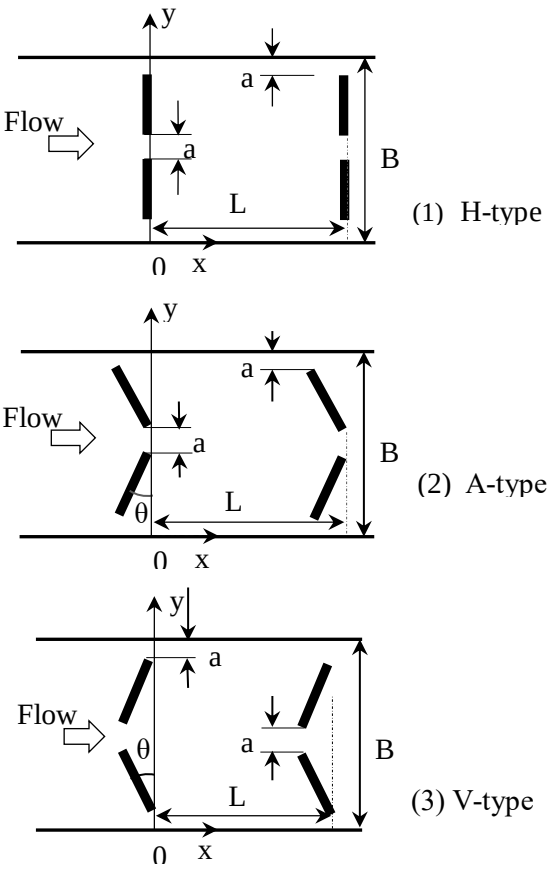

(a) Plan View

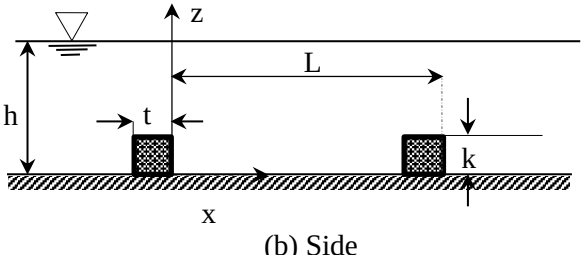

(b) Side

Fig.1 Experiment setup

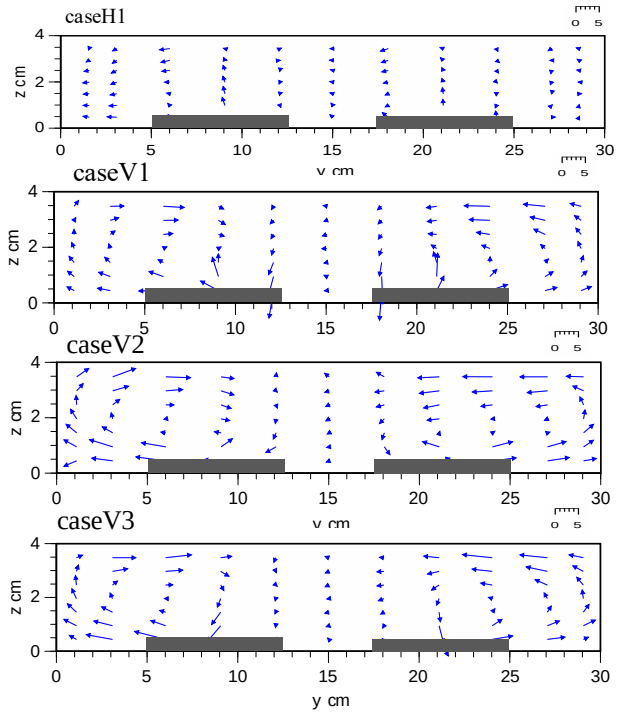

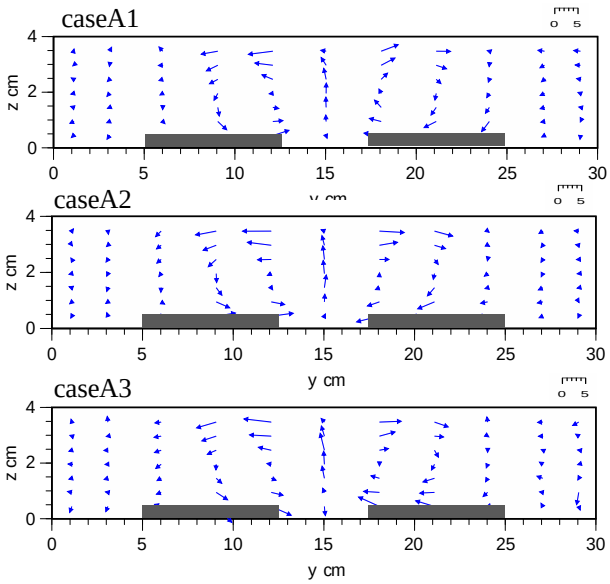

Fig.2 Secondary current

3. PIV Results and Discussion

(1) Secondary current

Fig.2 shows the vector distribution of the generated secondary currents at x=-3cm for H-type, V-type and A-type roughness arrangement. In the H-type roughness arrangement, *W* is a dominant component in the *VW* vector distribution causing multiple cellular motion of the secondary currents. For the cases where the roughness is skewed (A-type and V-type), a helicoid motion of secondary currents is generated. The upwelling and the downwelling component of the secondary current is at the mainstream and the near wall region respectively for the A-type strip arrangement and the opposite is true for the V-type strip arrangement. Furthermore, in A-type roughness arrangement, the transverse secondary flow (*V*) is characterized by convergence and divergence at the bed region and the free surface respectively with reference to the mainstream. On the other hand, the transverse flow (*V*) in the V-type is characterized by divergence and convergence at the bed region and the free surface respectively with reference to the mainstream. These distributions of the secondary flows are highly governed by the orientation of the skew angle of the roughness. The magnitudes of each component of the secondary current are discussed later in the text.

(2) Longitudinal Velocity *U* (cm/s).

Fig.3 shows the horizontal contour distribution of longitudinal velocity *U* at z=5mm. *U* is seen to have the same characteristics in both A-type and V-type roughness arrangement with different pattern of distribution. The peak value of *U* is seen at the upstream end of the

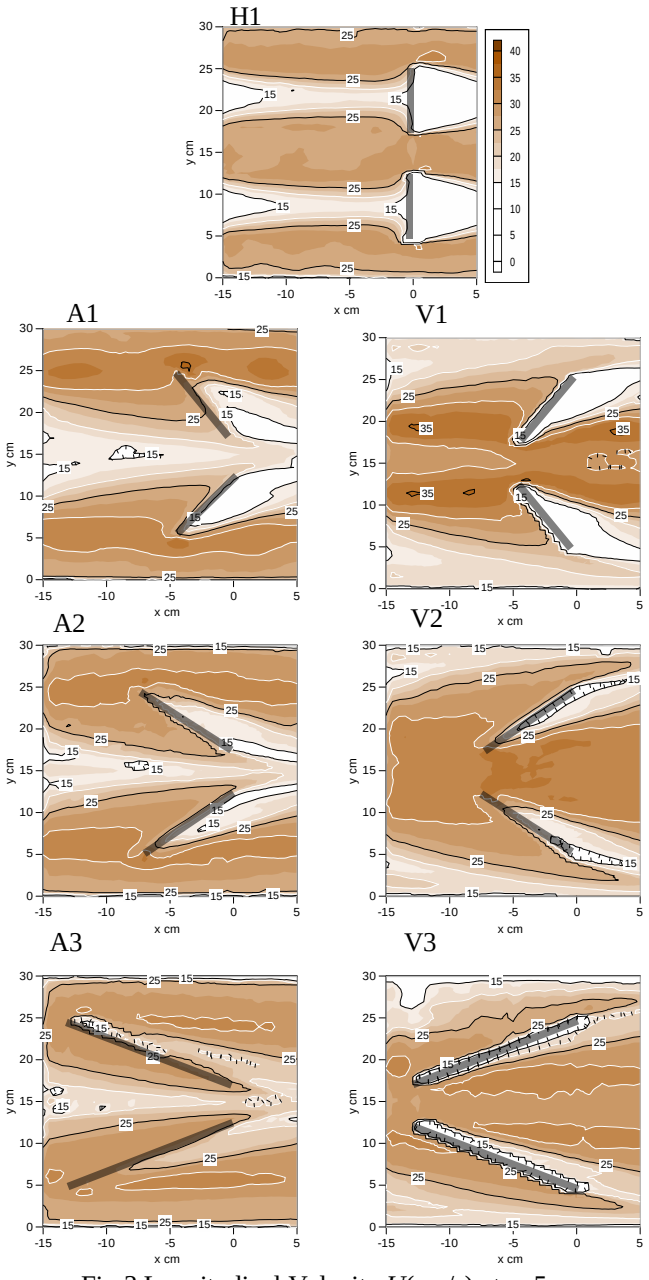

Fig.3 Longitudinal Velocity *U*(cm/s) at z=5mm

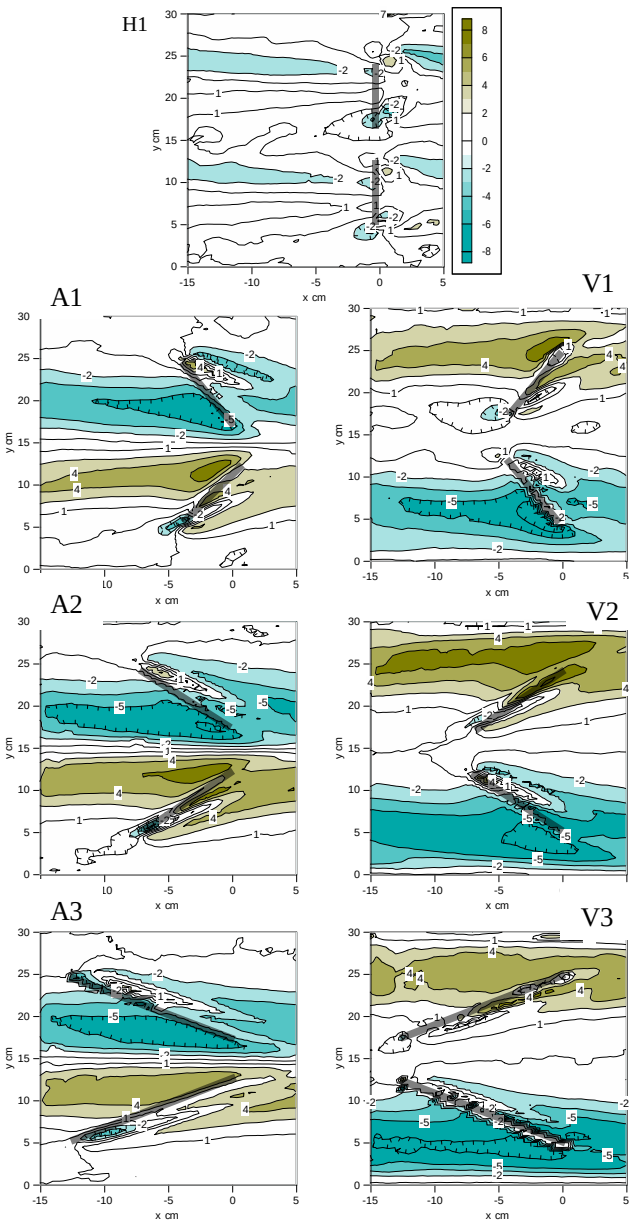

Fig.4 Transverse velocity V (cm/s) at z=5mm

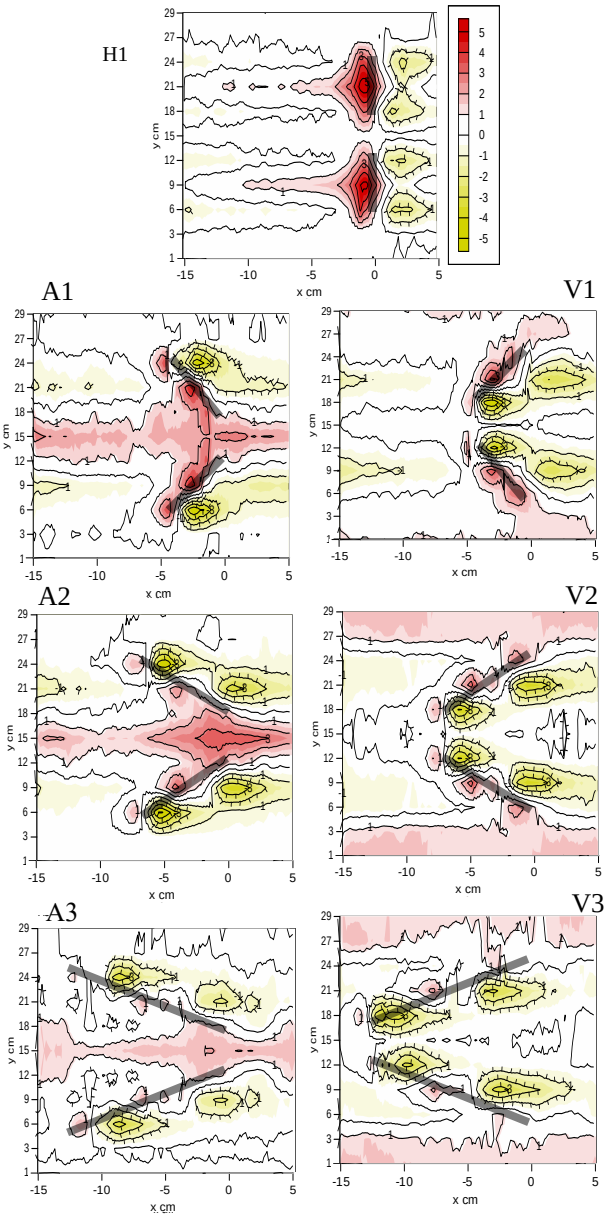

Fig.4 Vertical velocity W (cm/s) at z=10mm

roughness elements in all skewed cases. However, different skew angles affect the flow differently. The existence of the roughness elements in the channel tends to cause a resistance to the flow especially at the bed region. This resistance is seen to be very high in none skewed case than in the skewed cases. Comparing the effect of the skew angles, the resistance to flow decreases by widening the skew angle in both A-type & V-type. The distribution of U in the streamwise direction however, is nearly linear except at the bed in all cases.

(3) Vertical and transverse velocity distribution.

From the contour distribution of the transverse velocity V shown in Fig.4, in the case where the roughness is not skewed, the magnitude of the transverse flow is seen to be very small in comparison to the cases with skewed strip roughness. By changing the skew angle of the roughness elements, the magnitude of the transverse velocity component changes, with strong V in wider angles and decreases as the angle becomes narrow. This effect is seen in both the A-type and the V-type arrangement. Additionally, by changing the orientation of the same angle of the roughness from the A-type arrangement to the V-type arrangement, the magnitudes of V tend to decrease.

Fig.5 shows the distribution of the vertical velocity W at the bed region. For the case where the strips are not skewed, a very strong upflow is seen in front of the roughness due to the obstruction provided by the roughness. In both the A-type and the V-type arrangements, the upflow within the roughness region is sensitive to the skew angle of the roughness. The strength of the upflow in front of the roughness elements also shows how much resistance is caused to the flow. For the

upwelling component of the secondary currents, the magnitude of *W* increases from caseA1 to A2 then decrease in A3, similar behavior is seen in the V-type strip arrangement. In comparison, the upflow component of the secondary current seems to be higher in the A-type than the in the V- type. From the *VW* vector distribution in Fig.2, the downflow at the interface between the smooth and the rough region is clearly seen in the V-type than in the A-type strip arrangement. In the streamwise direction, *W* shows a nearly uniform distribution at the center and the near wall regions in all cases.

(4) Turbulence intensity. Fig.6 (d), (e) & (F) shows the horizontal (z=5mm) contour distribution of longitudinal turbulence intensities *u'*. High values of turbulence intensities are observed behind the upstream end of the roughness elements just at the elevation of the roughness top in all cases. However, this peak value reduces as the skew angle widens. Furthermore, the local effect of the strip elements on turbulence intensity is significant at the near bed region and diminishes towards the free surface in all cases.

4. Sediment Transport. In the case where the roughness is not skewed (caseH1), the zone of sediment transport cannot be control and deposition is seen all over the channel. However, the zone of sediment transport is seen to be different from one orientation of skew arrangement to another as shown in Fig.6 (a), (b) & (c). In the A-type, the sediment is highly deposited at the center of the channel. On the other hand, In the V-type, the sediment is highly deposited near the walls of the channel. These zones of sediment transport are due to the flow divergence or convergence at the bed region caused by the roughness elements. However, the volumes of these depositions are different for each type of roughness arrangement. From Fig.7, the rate of sediment transport is high in the none skewed case than in the skewed cases. Additionally, the transport of sediments in the skewed arrangements is highly dependent on the skew angle. The amount of sediments deposited reduces as the skew angle widens. This variation is only seen to be high in caseV1 than in caseV2 and V3. Similarly, caseA1 has more deposition than caseA2 and A3. This shows that more sediment is transported in the wider skew angles than the narrow skew angles.

5. Conclusion. From the experiments conducted, the following conclusions are deduced;

(1) Skewing the roughness elements proved to be effective in minimizing the resistance to flow. Wider skew angle of the roughness elements significantly reduces the resistance to the mainflow.

(2) The zone of sediment transport can be controlled by skewing the roughness elements and these zones are dependent on the skew direction of the roughness elements.

(3) The transport of sediments is maximized when the roughness elements are not skew. In cases with skewed roughness, the skew angle determines the rate of sediment transport.

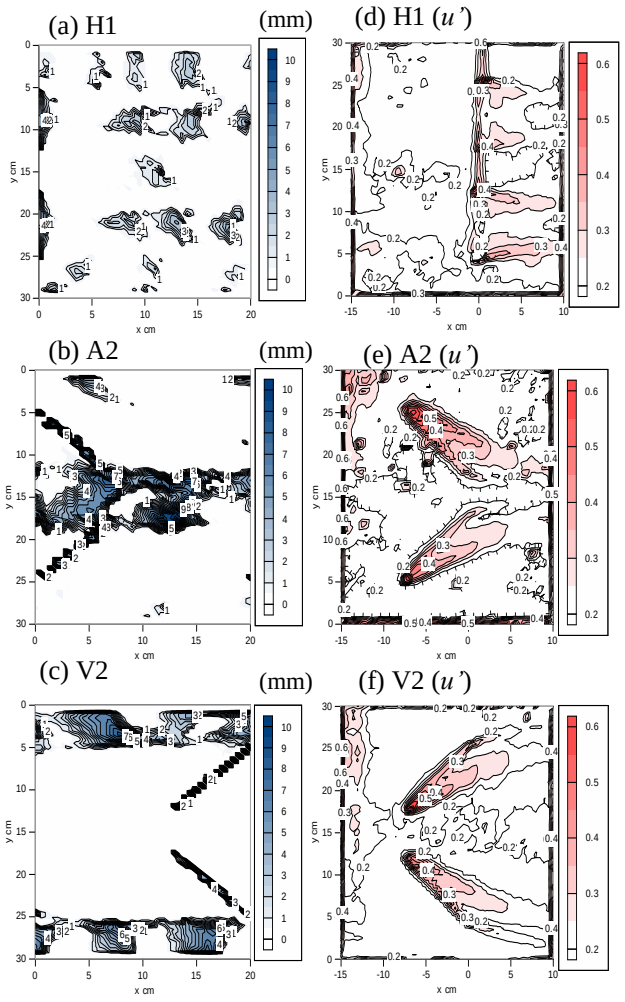

Fig.6

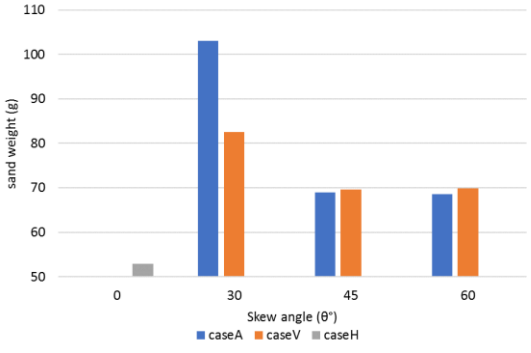

Fig.7 Sand quantities